Calculation of Error Rates for the Detection of Critical Situations in Road Traffic

Andreas Leich
German Aerospace Center (DLR)
Institute of Transportation Systems
Rutherfordstrasse 2, 12489 Berlin, Germany
Tel: +49 30 67055-409 Fax: +49 30 67055-291; Email: Andreas.Leich@dlr.de

Andreas Kendziorra
German Aerospace Center (DLR)
Institute of Transportation Systems
Rutherfordstrasse 2, 12489 Berlin, Germany
Tel: +49 30 67055-496 Fax: +49 30 67055-291; Email: Andreas.Kendziorra@dlr.de

Hagen Saul
German Aerospace Center (DLR)
Institute of Transportation Systems
Rutherfordstrasse 2, 12489 Berlin, Germany
Tel: +49 30 67055-7973 Fax: +49 30 67055-291; Email: Hagen.Saul@dlr.de

Ragna Hoffmann
German Aerospace Center (DLR)
Institute of Transportation Systems
Rutherfordstrasse 2, 12489 Berlin, Germany
Tel: +49 30 67055-268 Fax: +49 30 67055-291; Email: Ragna.Hoffmann@dlr.de

Word count: 5,433 words text + 5 tables/figures x 250 words (each) = 6,683 words

August 1st 2015

ABSTRACT

This article is a contribution to the development of methods for road safety analysis. A calculation scheme is derived for error rates of critical situations detected automatically using a road side stationary detector. A situation is classified as critical, if the time to collision is below some threshold. Calculated error rates are provided on different experiments with camera based vehicle detectors. The experiements demonstrate the best case of measurement accuracy that can be achieved using state of the art automated video surveillance technology. In the experiments, the false positive rate is five and four times higher than the true positive rate. This finding leads to the conclusion, that studies known from literature, stating there is correlation between the number of near crashes and real crashes should be faced with skepticism as long as no reliable information on error rates is provided.

Keywords: Surrogate Safety Measures, Time to Collision, Critical Situation, Near Crash, Error Rate

INTRODUCTION

There is a rising research interest in automatically identifying critical situations in road traffic. Critical situations comprise near crashes such as near collisions of following vehicles (rear-end conflicts as defined in (*1*)) or near collisions of vehicles that are in a turning or lane changing movement. Due to technological advances in the field of traffic sensing, more and more data can be collected on these relatively rare events. Results in this field have been published in (*2*), (*3*), (*4*) and others.

The availability of a corresponding data aquisition system paves the road to investigations on possible correlations between the number of near crashes and the number of real crashes in road traffic (*5*). In (*6*), a statistically significant relationship between the number of near-crashes and crashes was found by regression analysis of the data of 92 road intersections. The reliable identification of a critical situation is an important prerequisite for gaining reliable knowledge on this sort of coreherence.

In this paper, we deal with the error rates that occur, when critical situations are being identified automatically. A critical situation can be characterized by surrogate safety measures (*7*), as time to collision, post encroachment time and others. A situation is considered as critical, if the value of the safety measure drops below or rises above some predefined threshold. For the time to collision measure, a reasonable threshold often used in literature is $t_{tc} < 1{,}5s$ (*6, 8, 9, 10, 11*). While the detection error of the speed of road users in a video sequence has been well studied (e.g. see (*12*)) and attempts to improve the accuracy of speed estimation are known as well as performance evaluations exist (see (*13*)), very little is known on the error rate for the detection of a critical situation using such surrogate safety measure. Surrogate safety measures are being calculated from raw input data. For example the calculation of the time to collision requires speed and position data of the cars involved in the conflicting situation of a near crash.

In this paper, a closer look at the problem of error rate calculation is taken and a calculation scheme for the table of confusion of the detection process is presented. The table of confusion entries contain the elements as introduced in (*14*) - true-positive, false positive, true negative and false negative detection rates. Error propagation during the calculation of the surrogate safety measure and as well knowlegde about the probability distribution of the surrogate safety measure is accounted for. The motivation for the development of this scheme is to allow practitioners to raise requirements for sensors that are appropriate for the task of detecting a critical situation. The calculation scheme is applied to time to collision (TTC) measurements in rear-end conflicts detected from a stationary sensor and results presented. Implications for the usage of different types of stationary traffic detectors are discussed. Although the derivation of the scheme is focused on TTC measurements from a stationary sensor, the proposed method can be easily adapted to moving (in-vehicle) sensors and other surrogate safety measures.

This paper is organized in two sections. In the first section the computation scheme itself is derived. In this context assumptions for modeling of distance and velocity measurement errors and the approach to error rate calculation used in this paper are introduced in respective subsections. Another subsection is dedicated to the dataset for abtaining the knowledge on the distribution of TTC measurements from natural driving studies. The second section provides results. It presents table of confusion examples for given error magnitudes in the first subsection. In the second subsection, different versions of a video sensor are considered and the calculated confusion matrix values presented. The paper ends with conclusions and acknowledgements.

COMPUTATION OF TABLES OF CONFUSION

First, some requirements that have to be fulfilled by the sensor systems considered in this paper are stated. Here, the term *sensor system* does not just refer to the sensor, e.g. a camera. Instead, the whole system that is used to measure or determine velocities of objects and distances between objects is meant. For example, a camera together with a computer vision software and further software, which may include a filter (e.g. a Kalman filter or particle filter) for determing velocities, can be considered as a sensor system. The exact requirements for the sensor systems considered here are the following ones:

1. The sensor system measures the distance d between two detected objects O_1 and O_2. Clearly, O_1 and O_2 and have geometrical expansions. The distance between O_1 and O_2 is defined to be the closest distance of any two points p_1, p_2 for which p_1 belongs to O_1 and p_2 to O_2. In the case of two vehicles driving on a straight road, the distance would be approximataly the distance between the reer end of the leading vehicle and the front bumper of the following vehicle.
2. The error of the distance measurement is known in terms of the standard deviation σ_d. Here, it is assumed that the error of the distance measurement does not depend on the real value of the distance. That means, the standard deviation σ_d is constant for a sensor. In a section below, examples are presented on how to determine σ_d for certain sensors given some precision parameters.
3. The sensor system can measure the velocity v of a detected object.
4. The error of the velocity measurement is known in terms of the standard deviation σ_v. Analogously to the distance measurement, it is assumed that the error of the velocity measurement does not depend on the real value of the velocity. That means, the standard deviation σ_v is constant for a sensor.

Assumptions

For computing the tables of confusion, some further assumptions are introduced for simplicity reasons.

Distance Measurement

Regarding the distance measurement, it is assumed that, given a real distance value d^*, the distribution of the distance measurement is Gaussian with mean d^* and standard deviation σ_d.

Velocity Measurement

The same assumption as for the distance measurement is applied for the velocity measurement. That means, given a real velocity value v^*, the distribution of the velocity measurement is Gaussian with mean v^* and standard deviation σ_v. For computing TTC, one needs the velocity difference Δv between two objects. For that, it is assumed that the measurements of the velocities v_1 and v_2 of two detected objects O_1 and O_2 are independend (clearly, this is a fact and not just a simplification for most sensors). Therefore, the measurements of v_1 and v_2 are two independent Gaussian distributed random variables, which we denote by X_1 and X_2 and which have the same standard deviation σ_v. Clearly, the random variable $-X_1$, i.e. the measurement of $-v_1$, is also a Gaussian distributed random variable with standard deviation σ_v. Furthermore, $-X_1$ and X_2 are independent. As the sum of two independent Gaussian distributed random variables X, Y with standard deviations σ_x and σ_y is again a Gaussian distributed random variable with standard deviation $\sqrt{\sigma_x^2 + \sigma_y^2}$, the random variable $Z = X_2 + (-X_1)$, i.e. the measurement of the velocity difference $\Delta v = v_2 - v_1$, is a Gaussian distributed random variable with standard deviation

$$\sigma_{\Delta v} = \sqrt{\sigma_v^2 + \sigma_v^2} = \sqrt{2}\sigma_v \, . \tag{1}$$

TTC Measurement

When TTC will be mentioned in the following, it will always be assumed that it refers to two detected objects O_1, O_2 (the term *object* is prefered to the term *vehicle*, as pedestrians or other objects may be detected and considered as well), where O_1 moves towards O_2. Object O_1 will also be called the *following object* and O_2 the *leading object*. TTC fulfills then the equation $\mathrm{TTC} = -\frac{d}{\Delta v}$, where d is the distance between O_1 and O_2 and $\Delta v = v_2 - v_1$ the velocity difference, where v_i is the velocity of O_i for $i = 1{,}2$. Mostly, TTC is only defined for $\Delta v < 0$ in the literature, i.e. if the following object is faster than the leading object. However, here, TTC will also be defined for positive velocity differences. That means, also negative values for TTC will be considered. At first, this may appear ambigous, as one may interpret a negative TTC value as the time passed since a collision occured, what is clearly not the case for an object following a faster one. Obviously, this is a wrong interpretation of negative TTC values. A simple and sufficient interpretation is that negative TTC values always refer to uncritical situations because it implies a positive velocity difference (the leading object is faster), and if both objects continue moving with the current velocities and headings, a collision will never occur. The reason to consider negative TTC values is the following. It may occur that the real velocity difference of the detected objects is positive, which yiels by definition a negative TTC value, but the measured velocity difference is due to measurement errors negative, which yiels a positive measured TTC value. Depending on the treshold for critical TTC values, the measured value may be considered as critical. Hence, the measurement would be a false positive. Therefore, these situations have to be taken into account to determine the tables of confusion.

Now, the probability distribution of TTC will be described. The assumption is applied that the correlation coefficient $\rho_{d,\Delta v}$ of the distance measurement and the velocity difference measurement is known and constant. In the example calculations in the present paper, however, the correlation coefficient will mostly be assumed to be zero. The TTC is the quotient of two random variables thar are Gaussian distributed under the assumptions stated before. In (*15*), the analytical description of such a quotient random variable was given. For the present setting, the cumulative distibution function $F(t)$ of the random variable of measuring TTC, under the assumption that the real distance value is d^* and the real velocity difference value is Δv^*, has the following form[1]:

$$\begin{aligned} F(t) = \quad & L\left(\frac{d^* + t\Delta v^*}{\sigma_d \sigma_{\Delta v} a(t, \sigma_d, \sigma_{\Delta v}, \rho_{d,\Delta v})}, \frac{\Delta v}{\sigma_{\Delta v}}, \frac{t\sigma_{\Delta v} - \rho_{d,\Delta v}\sigma_d}{\sigma_d \sigma_{\Delta v} a(t, \sigma_d, \sigma_{\Delta v}, \rho_{d,\Delta v})}\right) \\ & + L\left(\frac{-t\Delta v^* - d^*}{\sigma_d \sigma_{\Delta v} a(t, \sigma_d, \sigma_{\Delta v}, \rho_{d,\Delta v})}, -\frac{\Delta v}{\sigma_{\Delta v}}, \frac{t\sigma_{\Delta v} - \rho_{d,\Delta v}\sigma_d}{\sigma_d \sigma_{\Delta v} a(t, \sigma_d, \sigma_{\Delta v}, \rho_{d,\Delta v})}\right), \end{aligned} \tag{2}$$

where

[1] For deriving equation (2) using the results of (*15*), the qotient random variable is assumed to be the random variable of measuring d devided by the random variable of measuring $-\Delta v$, i.e. the mean of the denominator random variable is $-\Delta v^*$.

$$a\left(t,\sigma_d,\sigma_{\Delta v},\rho_{d,\Delta v}\right)=\sqrt{\frac{t^2}{\sigma_d^2}-\frac{2t\rho_{d,\Delta v}}{\sigma_d\sigma_{\Delta v}}+\frac{1}{\sigma_{\Delta v}^2}} \tag{3}$$

and

$$L(h,k,\gamma)=\frac{1}{2\pi\sqrt{1-\gamma^2}}\int_h^\infty\int_k^\infty \exp\left(-\frac{x^2-2\gamma xy+y^2}{2(1-\gamma^2)}\right)\,dx\,dy\,. \tag{4}$$

Equation (4) is exactly the cumulative bivariate Gaussian distribution. For computing equation (4), numerical methods are required. Here, an implementation of Alan Genz's algorithm for computing multivariate Gaussian distributions (see (*16*)) was used.

Error Rate Computation

In this paper, a situation is considered as *positive* when the TTC value is critical and *negative* else. A TTC value is considered to be *critical* when it is non-negative and smaller or equal than a given threshold T_0, i.e. $0\leq \mathrm{TTC}\leq T_0$. Accordingly, a TTC value is considered to be *uncritical* if it is negative or larger than T_0. Therefore, a situation is considered to be

- a *true positive* (TP), if the real and the measured TTC value are critical,
- a *false positive* (FP), if the real TTC value is uncritical but the measured TTC value is critical,
- a *true negative* (TN), if the real and the measured TTC value are uncritical,
- a *false negative* (FN), if the real TTC value is critical but the measured TTC value is uncritical.

In terms of distance and veloctiy difference, a situation is critical if the velocity difference is negative and the distance is smaller or equal than $-T_0\Delta v$. Accordingly, a siutation is uncritical if the velocity difference is positive or the distance is larger than $-T_0\Delta v$. It is straight forward to reformulate the conditions of TP, FP, TN and FN in terms of distance and velocity difference.

To calculate a table of confusion, one has to know the frequency distribution of TTC to know how many situations are critical or uncritical in the road traffic. However, as the distribution of the measurement of TTC does depend on the real distance values and the real velocity difference value, this is not even sufficient. In fact, one has to know the bivariate joint frequency distribution of distance and velocity difference. For cunducting the investigations presented in this paper, such a distribution was known. The distribution was extraced from a naturalistc driving study (see (*17*)). The following subsection provides details on the computation of this distribution. For now, it is sufficient to know that this distribution is known and denoted by $h(d,\Delta v)$. In the following, the cumulative distribution function of measuring TTC in equation (12) will be denoted by $F_{d,\Delta v}(t)$ when the real distance value is d and the real velocity difference Δv. Then, the following equations yield the (unnormalized) frequencies of TP, FP, TN and FN:

$$q(\mathrm{TP})=\int_{-\infty}^{0}\int_{0}^{-T_0x}h(x,y)\left(F_{x,y}(T_0)-F_{x,y}(0)\right)\,dy\,dx \tag{5}$$

$$\begin{aligned}q(\mathrm{FP})=\;&\int_0^\infty\int_0^\infty h(x,y)\left(F_{x,y}(T_0)-F_{x,y}(0)\right)\,dy\,dx\\&+\int_{-\infty}^{0}\int_{-T_0x}^{\infty}h(x,y)\left(F_{x,y}(T_0)-F_{x,y}(0)\right)\,dy\,dx\end{aligned} \tag{6}$$

$$q(\mathrm{TN}) = \int_0^{\infty}\int_0^{\infty} h(x,y)\left(1 - F_{x,y}(T_0) + F_{x,y}(0)\right)\,dy\,dx + \int_{-\infty}^{0}\int_{-T_0 x}^{\infty} h(x,y)\left(1 - F_{x,y}(T_0) + F_{x,y}(0)\right)\,dy\,dx \quad (7)$$

$$q(\mathrm{FN}) = \int_{-\infty}^{0}\int_0^{-T_0 x} h(x,y)\left(1 - F_{x,y}(T_0) + F_{x,y}(0)\right)\,dy\,dx \quad (8)$$

For a better understanding, the equations will be explained. In equation (5), one integrates with respect to the velocity difference (here denoted by x) over the interval $(-\infty, 0)$, and with respect to the distance (here denoted by y) over the interval $(0, -T_0 x)$. Hence, one integrates over all pairs of distance and velocity difference values, such that the corresponding TTC value is critical. The integrand is exactly the product of the frequency of the pair (x, y), namely $h(x, y)$, and the probability that the measured TTC value is critical, namely $F_{x,y}(T_0) - F_{x,y}(0)$, under the assumption that the real distance is x and the real velocity difference y. Equation (6) is similar. One integrates over all pairs of distance and velocity difference values, such that the corresponding TTC value is uncritical. For that, one splits the integral into two terms. The first term consider all pairs, for which the velocity difference is positive, and the second term considers negative velocity differences and distances that yield a TTC value larger than T_0. The integrand is for both terms the same as in equation (5). Equations (7) and (8) and can be explained analogously, with the difference that the second factor of the integrands, namely $1 - F_{x,y}(T_0) + F_{x,y}(0)$, is the probability that the measured TTC value is uncritical.

For calculating the quantities contained in the table of confusion, one has to normalize these frequencies. That means, using the sum $S = q(\mathrm{TP}) + q(\mathrm{FP}) + q(\mathrm{TN}) + q(\mathrm{FN})$, the following frequencies yield a table of confusion:

$$p(\mathrm{TP}) = \frac{q(\mathrm{TP})}{S}, \quad p(\mathrm{FP}) = \frac{q(\mathrm{FP})}{S}, \quad p(\mathrm{TN}) = \frac{q(\mathrm{TN})}{S}, \quad p(\mathrm{FN}) = \frac{q(\mathrm{FN})}{S}. \quad (9)$$

Data set for distance and velocity difference distribution

The data for deriving the joint frequency distribution of the distance and the velocity difference was extracted from the *Intelligent Cruise Control Field Operational Test* (see (17)). This field operational test was conducted between 1996 and 1997 in Michigan, USA. For that, 10 vehicles were equipped with various sensors and instruments to measure driving dynanmic parameters as well as the distance to the preceding vehicle. The vehicles were given to 108 volunteers for two to five weeks, in which the data was constantly recorded. Although the purpose of the experiment was to investigate the comfort of adaptive cruise control (ACC), a sufficiently large amount of recorded trips without ACC was present. More precisely, there are 8690 trips of 102 drivers adding up to 1821 driving hours and 88,000 driving kilometres, in which no ACC was used. For determining the desired frequency distribution, only this kind of data was used.

Due to the measurment of the velocity of equipped vehicles and the distance to the preceeding vehicle, the velocity difference between the preceeding vehicle and the equipped vehicle could be computed as well. In Figure 1, the joint frequency distribution of the distance and the velocity difference can be seen. Further more, a resulting frequency distribution of TTC is displayed in Figure 2. Although, the distribution displayed in Figure 1 is used for the computation of the tables of confusion, and not the one in Figure 2, the latter figure provides an understanding of the distribution of critical and uncrtitical situations of in road traffic. In Figure 3, an enlarged view of small positive TTC values is shown to display more detailed the distribution of critical TTC values and positive uncritical TTC values (the distinction depends of course on the choice of the threshold T_0).

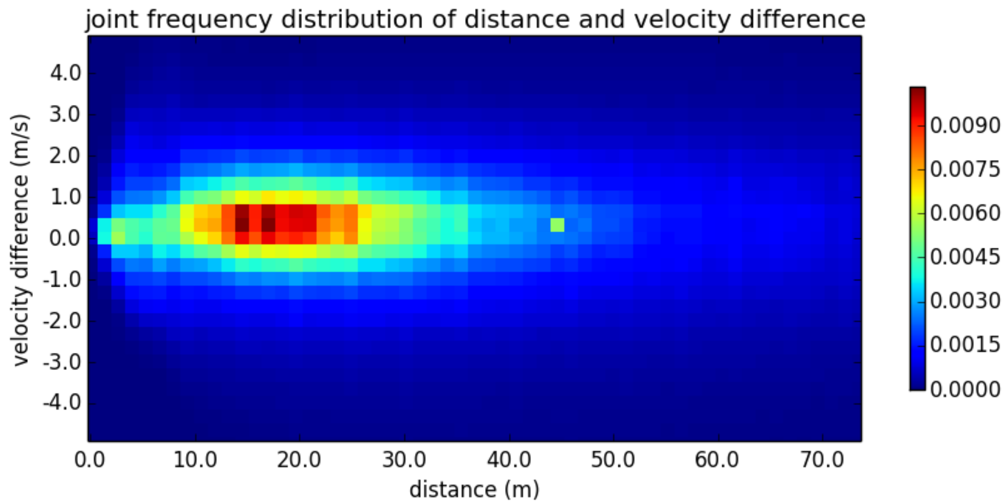

FIGURE 1 Joint frequency distribution of distance and velocity difference

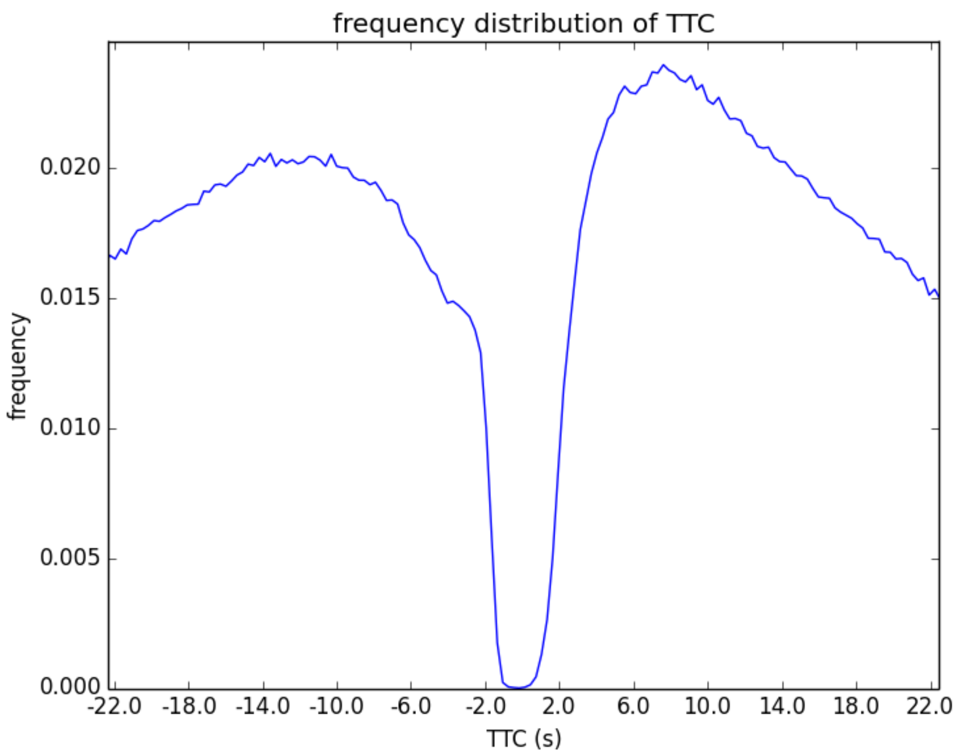

FIGURE 2 Frequency distribution of TTC; negatives TTC values, which imply a positive velocity difference, are included

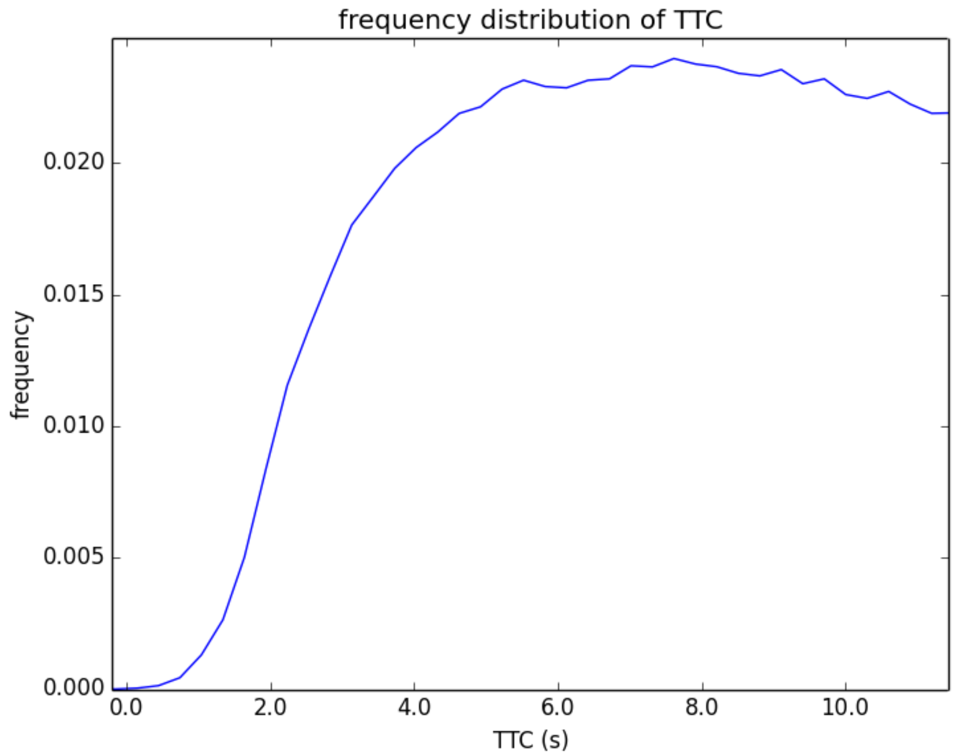

FIGURE 3 Frequency distribution of positive (and, depending on the threshold, possibly critical) TTC values

EXAMPLE CALCULATIONS

In this section, some example calculations for tables of confusion are presented. This includes some general examples using values for σ_d and σ_v that may be reasonable for sensor systems used in practize. These examples will be presented in the first subsection. In the second subsection, tables of confusions of sensor systems actullay used in practize will be presented.

Tables of confusion for reasonable values of σ_d and σ_v

In Table 1, one can see some tables of confusion for several values of σ_d and σ_v as well as for different values of the TTC threshold T_0. The correlation coefficient $\rho_{d,\Delta v}$ was always assumed to be zero. The values used for of σ_d and σ_v are assumed to be reasonable for sensor systems used in practice. The values used for T_0 correspond to thresholds used in the literature as well.

As one can see, the frequency of true positives is only for very few constellations larger than for false positives. As one might expect, this is the case for very small values of σ_d and σ_v.

TABLE 1 Tables of confusion for several values of σ_d and σ_v as well as for different values of the TTC threshold T_0; constellations, for which the frequency of true positives are larger than for false positives, are highlighted in green, all other constellations are highlighted in red; the correlation coefficient $\rho_{d,\Delta v}$ was always assumed to be zero

σ_d in m	σ_v in $\frac{m}{s}$	TTC threshold T_0 in s	$p(\text{TP})$	$p(\text{FP})$	$p(\text{TN})$	$p(\text{FN})$
0.1	0.01	0.5	0.022	0.009	99.956	0.013
1.0	0.01	0.5	0.003	0.059	99.906	0.032
10.0	0.01	0.5	0.000	0.376	99.508	0.035
0.1	0.1	0.5	0.022	0.010	99.945	0.014
1.0	0.1	0.5	0.003	0.060	99.905	0.032
10.0	0.1	0.5	0.000	0.378	99.586	0.035
0.1	1.0	0.5	0.018	0.052	99.912	0.017
1.0	1.0	0.5	0.006	0.142	99.823	0.030
10.0	1.0	0.5	0.001	0.587	99.378	0.035
0.1	0.01	1.0	0.059	0.005	99.899	0.037
1.0	0.01	1.0	0.018	0.133	99.770	0.079
10.0	0.01	1.0	0.002	0.759	99.145	0.095
0.1	0.1	1.0	0.058	0.007	99.896	0.038
1.0	0.1	1.0	0.018	0.136	99.768	0.078
10.0	0.1	1.0	0.002	0.763	99.141	0.095
0.1	1.0	1.0	0.051	0.232	99.671	0.046
1.0	1.0	1.0	0.029	0.356	99.547	0.067
10.0	1.0	1.0	0.004	1.181	98.722	0.093
0.1	0.01	2.0	0.380	0.004	99.582	0.034
1.0	0.01	2.0	0.221	0.284	99.302	0.193
10.0	0.01	2.0	0.037	1.521	98.065	0.377
0.1	0.1	2.0	0.343	0.033	99.553	0.071
1.0	0.1	2.0	0.221	0.294	99.292	0.193
10.0	0.1	2.0	0.037	1.529	98.057	0.377
0.1	1.0	2.0	0.243	0.850	98.736	0.171
1.0	1.0	2.0	0.212	0.957	98.629	0.202
10.0	1.0	2.0	0.044	2.378	97.208	0.370

Table of confusion of a viodeo based sensor system

In the following, two experiments conducted with camera sensor systems are presented. The sensor systms are capable of detecting and tracking objects for determining the road user's position and velocity. Therefore, such sensor systms can be used for deriving surrogate safety measures like TTC. The experiments demonstrate the capability and limitations of an automatic video surveillance algorithm in this context.

Experiment 1

The results of the first experiment were already partly presented in (*18*). In three scenarios, a single car equipped with a differential-GPS-receiver was observed with a camera. In the three test drives, the car passes pylones describing a chicane at different target velocities, i.e. 30 km/h and 50 km/h. The distance of the vehicle to the camera remained within a narrow range of approximately 10-15m. Thus, this experiment provides stable and optimal conditions for localizing the vehicle by camera and computer vision and in this way represents the best case for this means of sensor.

The measurement process involves fitting a 3D wire model onto the car in the image in every video frame. The model's parameters were especially adapted to the test vehicle in order to fit the vehicle's hull best. As the fitting converges, the gravity point of the model's ground face is taken as the vehicle's position measurement. The vehicle position is then tracked by a Kalman filter. For additional information of how the measurements are taken, see (*18*).

The results of the image processing methods are validated by comparing them to high-precision DGPS positions from the observed vehicle. Only the position errors have been considered, since the altitude is assumed to be on the planar road surface. The intrinsic camera orientation (focal length, lens distortion etc.) has been calibrated in advance in the laboratory, while the extrinsic orientation had been calibrated on site using GPS measured ground control points. The reference data set (groundtruth) was obtained by using the observed car's inertial measurement system iDIS-FMS from the manufacturer iMAR which was created for motion analysis of cars, ships, airplanes. It records altitude angles, velocities and accelerations as well as GPS positions. Using post-processing and differential GPS (DGPS), iMAR claims to provide an accuracy of better than 1 cm in positioning. Unfortunately, the current accuracy values were not recorded during the tests. However, both DGPS and post processing have been used, such that a precision of 5 cm is assumed. The corresponding points (groundtruth position representing the expected and true position and the estimation of the measurement), which have to be comparable, are determined for evaluation by linearly interpolating the positions of the two closest groundtruth-points. Thus, the measurements and the groundtruth are time-registered. The error of the position measurement along the direction of motion in terms of the standard deviation is $\sigma_x = 0.17\,m$. Regarding the velocity, the standard deviation is $\sigma_v = 1.36\frac{m}{s}$. The correlation coefficient is $\rho_{d,\Delta v} = 0.12$.

The measurements of the position of a vehicle referred so far to its middle point. However, for determining the distance between two vehicles, one is interested in the position of the rear end of the leading vehicle and the front bumper of the following vehicle. The length vehicles must to be determined therefore. In this example, an average length of vehicles and the standard deviation of these lengths will be used. By parsing inductive loop data protocols with a sample size of $4.5 \cdot 10^6$ vehicles, a mean length of $\bar{l} = 4.06\,m$ and the standard deviation $\sigma_l = 0.63\,m$ could be determined. For two vehicles O_1, O_2 with positions x_1, x_2 and lengths l_1, l_2, where O_1follows O_2, the distance d between the rear end of $O_2$and the front bumper of O_1 fulfills

$$d = x_2 - \frac{l_2}{2} - x_1 + \frac{l_1}{2}.$$

As l_1, l_2 will be measured by simply guessing to be $\bar{l}$, the measurement of d has the standard deviation

$$\sigma_d = \sqrt{\sigma_x^2 + \left(\frac{\sigma_l}{2}\right)^2 + \sigma_x^2 + \left(\frac{\sigma_l}{2}\right)^2} = \sqrt{2\sigma_x^2 + \frac{1}{2}\sigma_l^2},$$

yielding in this setting the value

$$\sigma_d = \sqrt{2 \cdot 0.17^2\, m^2 + \frac{1}{2} 0.63^2\, m^2} = 0.51\, m\,.$$

Using the scheme developed here, the following table of confusion is calculated, where the TTC threshold $T_0 = 2.0\ s$ was used:

$$p(\mathrm{TP}) = 0.233\%\,, \quad p(\mathrm{FP}) = 1.253\%\,, \quad p(\mathrm{TN}) = 98.333\%\,, \quad p(\mathrm{FN}) = 0.181\%\,.$$

The frequency of false postives is about five times larger than the one of true positves. Even if one would neglect the measurement error of guessing the length, i.e. assuming $\sigma_l = 0$, one would get $\sigma_d = 0.24\ m$, what results in the following table of confusion:

$$p(\mathrm{TP}) = 0.235\%\,, \quad p(\mathrm{FP}) = 1.255\%\,, \quad p(\mathrm{TN}) = 98.331\%\,, \quad p(\mathrm{FN}) = 0.179\%\,.$$

One can see, that, given this relatively large value for σ_v, even a precise position measurement does not improve the result much.

Experiment 2

The second experiment was conducted within the scope of the project OptiSilk (*19*), studying the safety of road users at an unguarded railway crossing. Due to existing specifications of the project, different algorithms compared to experiment 1 for object detection, tracking and for acquisition of groundtruth were used. The evaluated scene represents realistic conditions with normal traffic, e.g. bulks of road users in succession and occluding each other. Additonally, the road is along the visual axis of the camera enabling to determine the errors of position and velocity in dependence from the distance to the sensor.

In order to evaluate the traffic safety at the test site, in total three hours of video data have been recorded, of which approximately half an hour is annotated with groundtruth object data. The groundtruth data is acquired by annotating the video frame-wise, i.e. setting a bounding box for each object in the scene, resulting in sufficiently precise trajectories in near range, but also a lack of precision in far distance, which was more than 100m in this scene. As in experiment 1, the exterior orientation projecting the camera coordinates into world coordinates is determined by using GPS measured ground control points and the intrinsic camera orientation has been calibrated in advance in the laboratory likewise. The automatic object detetection is done at manually set ellipse areas, capturing and detecting vehicles at every lane for both directions of the street when vehicles pass by. For this purpose a Support Vector Machine is trained with Histograms of oriented Gradients of different classes of vehicles (e.g. car, lorry, etc.). If an object is detected, the tracking algorithm is triggered. The tracking algorithm presented in (*19*) works as follows: The global maximum of the motion of the optical flow within an ellipse in the image, the region of interest (ROI), is determined using the spatial and temporal gradients at all pixel positions in the ROI. Using this approach the velocity measurements are assumed to be more accurate than the position obtained by projecting the gravity point of the ellipsis on the street.

The evaluation is done by associating pairs of trajectories—for each groundtruth trajectory acquired by annotation, a corresponding automatically determined trajectory by the tracking algorithm mentioned in the previous subsection is found. Note that another algorithm may require finding several trajectories if a vehicle could not be tracked the whole stretch. Such an algorithm would produce chopped vehicle trajectories. After associating corresponding trajectory pairs, simultaneous trajectory points are determined. For every trajectory point pair the difference between the measured position and velocity along the driving direction and the expected groundtruth parameters is calculated with the following results: The error for the position measurement in terms of the standard deviation is $\sigma_x = 0.515\ m$ and the error of the velocity measurement $\sigma_v = 1.1\,\frac{m}{s}$. Analougously to experiment 1, the standard deviation for the distance measurement is

$$\sigma_d = \sqrt{2 \cdot 0.515^2\ m^2 + \frac{1}{2} 0.63^2\ m^2} = 0.85\ m\ ,$$

yielding the following table of confusion assuming a correlation of zero:

$$p(\mathrm{TP}) = 0.228\%\ , \quad p(\mathrm{FP}) = 1.002\%\ , \quad p(\mathrm{TN}) = 98.583\%\ , \quad p(\mathrm{FN}) = 0.186\%\ .$$

In this case, the number of false positives is about four times the number of true positives, which is better than in the first experiment, but assumably too unprecise to prove a correlation between numbers of near-crashes and real crashes.

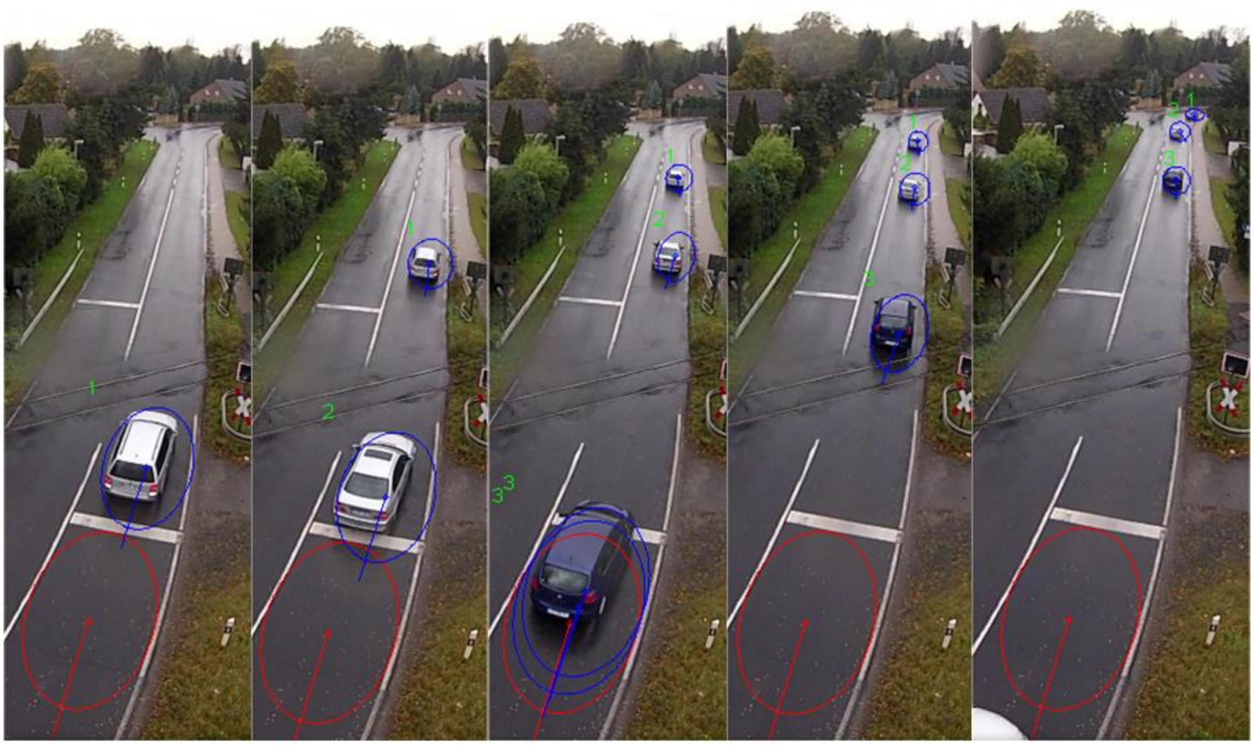

FIGURE 4 Screen shots from the detection system used in experiment 2. The red ellipse represents the detection area, the blue ellipses represent the objects being tracked

CONCLUSIONS

A means for error rate calculation for the TTC based detection on critical situations was derived in this paper. The respective calculation scheme is based on the assumption that the error distribution of the quantities involved in TTC computation is Gaussian and the probability density distribution of TTC in traffic is known. In implementation was presented based on probablibily density data of TTCs collected in a natural driving study.

Error rates were calculated for two experimental setups representing automated video based surveillance systems with state of the art image processing algorithms. It was observed, that the false positive rates were four to five times higher than the true positive rates. The implication is that such systems should be expected to produce a high number of false alarms. Manual post processing of the detected critical situations is a mandatory exercise in studies on surrogate safery measures, as was done in (*3*). Results, provided to the research community claiming that the correlation coefficient between the numbers of near crashes and real crashes has a certain value, should be interpreted carefully and revisited, as far as reliable information on respective error rates on the quantities involved is not available.

The calculation scheme is a theoretic concept, which as well needs to be proven by some sort of automatically collected large scale ground truth data. By now, this is not available to the authors. It is subject to further research to conduct a field study in this regard.

ACKNOWLEDGMENTS

The funding for this project has been provided by DLR's project I.MoVe.

REFERENCES

1. Perkins, S. R., and Harris, J I. *Criteria for Traffic Conflict Characteristics, Signalized Intersections.* Research Laboratories, General Motors Corporation, 1967.
2. Saunier, N., Sayed, T., and Ismail, K. Large-scale automated analysis of vehicle interactions and collisions. In: *Transportation Research Record: Journal of the Transportation Research Board 2147* (2010), pp. 42–50.
3. Twaddle, H., Schendzielorz, T., Fakler, O., and Amini, S. Use of automated video analysis for the evaluation of bicycle movement and interaction. In *Proc. SPIE 9026, Video Surveillance and Transportation Imaging Applications 2014*. SPIE, 2014.
4. Ardö, H., Nilsson, M., and Laureshyn, A. *Superpixel based road user tracker.* 2013.
5. Guo F., Klauer, S. G., McGill, M. T., Dingus, T. A. *Evaluating the relationship between near-crashes and crashes: Can near-crashes serve as a surrogate safety metric for crashes?* U.S. Department of Transportation, National Highway Traffic Safety AdministrationIn: (2010).
6. Sayed, T., and Zein, S. (1999). Traffic conflict standards for intersections. In *Transportation Planning and Technology*, 22(4), 309-323.
7. Tarko, A., Davis, G., Saunier, N., Sayed, T., & Washington, S. (2009). *Surrogate measures of safety.* White paper, ANB20 (3) Subcommittee on Surrogate Measures of Safety.
8. Hupfer, C. *Computergestützte Videobildverarbeitung zur Verkehrssicherheitsarbeit - am Beispiel von Fußgängerquerungen an städtischen Hauptverkehrsstraßen.* Dissertation, Technische Universität Kaiserslautern, Institut für Mobilität und Verkehr, Grüne Reihe, Nr. 40,1998
9. Stevanovic, A., Stevanovic, J. and Kergaye, C. Optimisation of traffic signal timings based on surrogate safety. In *Transportation Research Part C: Emerging Technologies*, 32, pp. 159-178, 2013

10. Hydén, C.: *The development of a method for traffic safety evaluation: The Swedish Conflict Technique.* Lund University of Technology, Lund,1987
11. Van der Horst, A.R.A.: *A time-based analysis of road user behavior in normal and critical encounters.* Dissertation, Delft University of Technology, 1990
12. Anderson-Trocmé, P., Stipancic, J., Miranda-Moreno, L. and Saunier, N. Performance evaluation and error segregation of video-collected traffic speed data. *Transportation Research Board Annual Meeting Compendium of Papers.* 2015, pp. 15–1337.
13. Wu, W., Kozitsky, V., Hoover, M. E., Loce, R., and Todd Jackson, D. M. Vehicle speed estimation using a monocular camera. In *IS&T/SPIE Electronic Imaging.* International Society for Optics and Photonics. 2015, pp. 940704–940704
14. Fawcett, T. An introduction to ROC analysis. In *Pattern recognition letters 27.8* (2006), pp. 861– 874.
15. Hinkley, D. V. (1969). On the ratio of two correlated normal random variables. *Biometrika*, 56(3), 635-639.
16. Genz, A. (1992). Numerical computation of multivariate normal probabilities. *Journal of computational and graphical statistics*, 1(2), 141-149.
17. Fancher, P., Ervin, R., Sayer, J., Hagan, M., Bogard, S., Bareket, Z., Mefford, M., and Haugen, J. (1998). *Intelligent cruise control field operational test*. Final Report. U.S. Department of Transportation National Highway Traffic Safety Administration.
18. Kozempel, K., Saul, H., Haberjahn, M. & Kaschwich, C.(2014). A Comparison of Trajectories and Vehicle Dynamics Acquired by High Precision GPS and Contemporary Methods of Digital Image Processing. *Urban Transport XX*, pp. 381-391.
19. Leich, A., Junghans, M., Kozempel, K., & Saul, H. (2015). Road user tracker based on robust regression with GNC and preconditioning. In *IS&T/SPIE Electronic Imaging* (pp. 940702-940702). International Society for Optics and Photonics.